SIMULATION OF Q-TENSOR FIELDS WITH CONSTANT ORIENTATIONAL ORDER PARAMETER IN THE THEORY OF UNIAXIAL NEMATIC LIQUID CRYSTALS

SÖREN BARTELS AND ALEXANDER RAISCH

Abstract. We propose a practical finite element method for the simulation of uniaxial nematic liquid crystals with a constant order parameter. A monotonicity result for Q-tensor fields is derived under the assumption that the underlying triangulation is weakly acute. Using this monotonicity argument we show the stability of a gradient flow type algorithm and prove the converge of outputs to discrete stable configurations as the stopping parameter of the algorithm tends to zero. Numerical experiments with singularities illustrate the performance of the algorithm. Furthermore, we examine numerically the difference of orientable and non-orientable stable configurations of liquid crystals in a planar twodimensional domain and on a curved surface. As an application, we examine tangential line fields on the torus and show that there exist orientable and non-orientable stable states with comparing Landau-de Gennes energy and regions with different tilts of the molecules.

1. Introduction and derivation of the mathematical setting

The modelling of liquid crystals has attracted considerable attention among mathematicians in the last decade [1, 2, 3, 4, 10, 12, 13, 14, 18] Starting with the prediction of stationary configurations for the classical Oseen-Frank model right through to studies of the motion of liquid crystals governed by the Ericksen-Leslie model. In recent years it has become more popular to use Q-tensors to describe nematic liquid crystals. One of the main features of this theory is that it captures symmetries of the molecules which are not seen by the classical models. In [4] this feature is examined analytically and examples are constructed to show that there are settings where the classical theory misses stationary configurations that are energetically more favorable for the liquid crystal. The analysis leads directly to topological issues and the question of the orientability of given line fields. It is the aim of this paper to devise numerical methods for both models and to understand relations between them. Following [4], the molecules of a nematic liquid crystal can be thought of as rod-like molecules with two ends indistinguishable from each other, a center of mass at a position $x \in \Omega$ and a certain direction in space. Here and in the rest of this report $\Omega \subset \mathbb{R}^d$ $(d = 2, 3)$ is a bounded Lipschitz domain representing the vessel. For a well-defined macroscopic variable describing the crystal it is required to use statistical averages of the molecular orientation of the crystal. We let $\mathcal{L}(\mathbb{S}^2)$ denote the family of Lebesgue measurable subsets of the unit sphere $\mathbb{S}^2$, and assign to every point $x \in \Omega$ a probability measure $\mu(x, \cdot) : \mathcal{L}(\mathbb{S}^2) \to [0, 1]$ so that $\mu(x, \{n\})$ is the probability of the crystal at the point x to point in direction n. Since the molecules admit the so-called head-to-tail symmetry we have that $\mu(x, A) = \mu(x, -A)$ for every $x \in \Omega$ and every $A \subset \mathbb{S}^2$. This property yields that all odd moments of μ must vanish. The lowest order even moment, which is assumed to be the most important quantity for describing liquid crystals, is given by

$$M_{ij}(x) = \int_{\mathbb{S}^2} p_i p_j \,\mathrm{d}\mu(x, p), \quad i, j = 1, 2, 3, \; x \in \Omega$$

The matrix valued function $M : \Omega \to \mathbb{R}^{3\times 3}$ has the properties

$$M = M^T, \; M \geq 0 \text{ and } \operatorname{tr} M = 1.$$

We define the trace-free *de Gennes* order parameter tensor $Q := M - \frac{1}{3}\mathrm{id}$ and distinguish three different cases: (1) If Q has three equal eigenvalues then $Q = 0$ and we call the crystal isotropic, that means, the orientation of the molecules is totally random. (2) If Q has two equal eigenvalues, then the crystal is called uniaxial and Q admits a representation of the form

$$Q = s(n \otimes n - \frac{1}{3}\mathrm{id}),$$

Date: November 12, 2012.

where $n \in \mathbb{S}^2$ is the optical axis and $s \in \mathbb{R}$ is the orientational order parameter. The orientational order s takes values between $s = -\frac{1}{2}$ (molecules are planar oriented and perpendicular to the optical axis) and $s = 1$ (perfect alignment of the molecules with the optical axis). The uniaxial case is characteristic for nematics and cholesterics. (3) If Q has three distinct eigenvalues, then the crystal is called biaxial. In practice, however, it is observed that liquid crystals are uniaxial almost everywhere with a constant order parameter s between 0.6 and 0.8. We therefore restrict ourselves to the case $Q(x) = s(n(x) \otimes n(x) - \frac{1}{3}\mathrm{id})$ with s constant and $n(x) \in \mathbb{S}^2$ for $x \in \Omega$. When we talk about the classical Oseen-Frank model we think of the liquid crystal being described simply by a director field $n : \Omega \to \mathbb{S}^2$, the optical axis. As in our simplified Q-tensor model we assume a constant orientational order parameter. More details for a substantial treatment of this derivation and an introduction to the classical model can be found in [13, 18].

A model to predict stable liquid crystal configurations is to compute stationary points of the energy

$$E_{OF}(n) := \int_\Omega W(n, \nabla n)\,\mathrm{d}x := \int_\Omega k_1|\mathrm{div}\, n|^2 + k_2|n \cdot \mathrm{curl}\, n|^2 + k_3|n \times \mathrm{curl}\, n|^2 + (k_2 + k_4)(|\nabla n|^2 - |\mathrm{div}\, n|^2)\,\mathrm{d}x,$$

with elastic constants k_1, k_2, k_3, k_4. It is possible to choose a function Ψ, depending on the tensor $Q = s(n \otimes n - \frac{1}{3}\mathrm{id})$, so that the energy density W can be expressed as

$$W(n, \nabla n) = \Psi(Q, \nabla Q),$$

see [4] for details. We will refer to the constrained Landau-de Gennes theory when considering the energy density Ψ and de Gennes order parameter tensors. If $Q = s(n \otimes n - \frac{1}{3}\mathrm{id})$ almost everywhere in Ω with $n : \Omega \to \mathbb{S}^2$ then

$$E_{OF}(n) = \int_\Omega W(n, \nabla n)\,\mathrm{d}x = \int_\Omega \Psi(Q, \nabla Q)\,\mathrm{d}x =: E_{LdG}(Q).$$

and the Landau-de Gennes theory can be interpreted as a generalization of the classical Oseen-Frank model. In the most simple (equal constant) setting E_{OF} reduces to the standard Dirichlet energy for functions with values in $\mathbb{S}^2$ and the fact that

$$|\nabla(n \otimes n)|^2 = 2|\nabla n|^2$$

yields

$$|\nabla Q|^2 = s^2|\nabla(n \otimes n - \frac{1}{3}\mathrm{id})|^2 = s^2|\nabla(n \otimes n)|^2 = 2s^2|\nabla n|^2.$$

Thus, if $Q = s(n \otimes n - \frac{1}{3}\mathrm{id})$ in Ω then

$$\frac{1}{2}\int_\Omega |\nabla n|^2\,\mathrm{d}x = \frac{1}{4s^2}\int_\Omega |\nabla Q|^2\,\mathrm{d}x$$

and E_{LdG} is a multiple of the Dirichlet energy for functions with values in

$$\widetilde{\mathbb{L}}^2 := \left\{ A \in \mathbb{R}^{3\times 3} : \exists n \in \mathbb{S}^2, \exists s \in [-1/2, 1] : A = s(n \otimes n - \frac{1}{3}\mathrm{id}) \right\}.$$

Since we are interested only in the Dirichlet energy it is convenient to set $s = 1$ and replace $\widetilde{\mathbb{L}}^2$ by the submanifold

$$\mathbb{L}^2 := \left\{ A \in \mathbb{R}^{3\times 3} : \exists n \in \mathbb{S}^2, A = n \otimes n \right\}.$$

We observe that $\mathbb{L}^2$ can be identified with the real projective space $\mathbb{R}P^2 = \mathbb{S}/\pm$ using the map

$$b : \mathbb{L}^2 \to \mathbb{R}P^2,\ A = n \otimes n \mapsto \{n, -n\}.$$

It is possible to endow $\mathbb{L}$ with a Riemannian structure so that it is a Riemannian manifold. Throughout this work we refer to the Oseen-Frank energy as

$$E_{OF} : W^{1,2}(\Omega, \mathbb{S}^2) \to \mathbb{R},\ n \mapsto \frac{1}{2}\int_\Omega |\nabla n|^2\,\mathrm{d}x$$

and to the Landau-de Gennes energy as

$$E_{LdG} : W^{1,2}(\Omega, \mathbb{L}^2) \to \mathbb{R},\ Q \mapsto \frac{1}{4}\int_\Omega |\nabla Q|^2\,\mathrm{d}x.$$

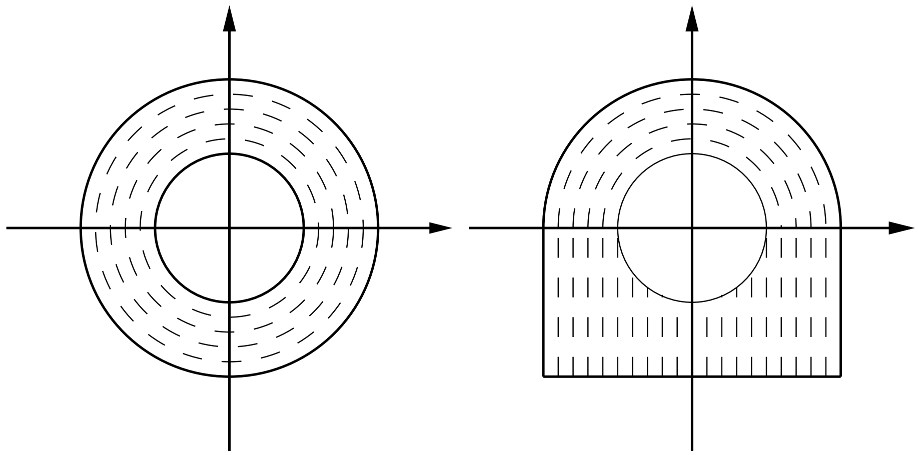

FIGURE 1. Orientable and non-orientable line fields in the plane.

We will call stationary points of E_{OF} *harmonic director fields* and stationary points of E_{LdG} will be called Q *harmonic tensor fields* or *harmonic line fields.*

The molecules of the liquid crystal tend to align themselves parallel to the boundary when they are in contact with other materials. These boundary conditions are often referred to as partial constraint or planar anchoring conditions. When the surface is worked in a special manner the liquid crystal aligns with the treatment and can be specified. In this case one speaks about strong or homeotropic anchoring conditions. In our twodimensional simulation in Section 6 we will also allow for Neumann boundary conditions in parts of $\partial\Omega$. They are not motivated by the physics but simplify the computations and help us to underline the difference of the Oseen-Frank and the Landau-de Gennes theory.

Clearly every $n \in W^{1,2}(\Omega, \mathbb{S}^2)$ defines a map $Q = n \otimes n \in W^{1,2}(\Omega, \mathbb{L}^2)$. The interesting question is whether the converse statement holds in the sense that for $Q \in W^{1,2}(\Omega, \mathbb{L}^2)$ there exists $n \in W^{1,2}(\Omega, \mathbb{S}^2)$ such that $Q = n \otimes n$. This is true in some situations, cf. left plot in Figure 1, but in general this is not the case as can be seen in the right plot of Figure 1. In the latter one we set $G_1 = (-1, 1) \times (-1, 0)$, $G_2 = B_1(0) \cap \{x_2 \geq 0\}$ and $G = G_1 \cup G_2 \setminus B_{1/2}(0)$. We define the field

$$n(x) = \begin{cases} (-x_2, x_1, 0) & \text{if } x \in G \cap \{x_2 \geq 0\} \\ (0, 1, 0) & \text{if } x \in G \cap \{x_2 < 0\} \end{cases} .$$

Then $Q := n \otimes n \in W^{1,2}(\Omega, \mathbb{L}^2)$ and if $Q = \tilde{n} \otimes \tilde{n}$ then $\tilde{n} = \pm n$ almost everywhere but there is no way to construct a vector field $\widetilde{n}$ without any jump in Ω and satisfying $\widetilde{n}(x) = n(x)$ or $\widetilde{n}(x) = -n(x)$ for almost every $x \in \Omega$. These observations motivate the following definition.

Definition 1.1. *We say that a line field $Q \in W^{1,2}(\Omega, \mathbb{L}^2)$ is* orientable *if there exists $n \in W^{1,2}(\Omega, \mathbb{S}^2)$ such that $Q = n \otimes n$ a.e. in Ω. Otherwise Q is called* non-orientable.

In the discrete setting we work with piecewise affine tensor fields Q_h that satisfy $Q_h(z) \in \mathbb{L}^2$ for all nodes z in the triangulation. Analogously we work with discrete vector fields n_h which are piecewise affine and satisfy $n_h(z) \in \mathbb{S}^2$. Thus, there always exists a discrete director field n_h such that $Q_h(z) = n_h(z) \otimes n_h(z)$ for all nodes z and for $h > 0$ fixed we have that $n_h \in W^{1,2}(G, \mathbb{R}^3)$. From this it follows that we can always assign a discrete director field to a discrete line field and every line field is orientable in a discrete sense but the identity $|\nabla Q_h|^2 = 2|\nabla n_h|^2$ may be violated. Thus, using the energies E_{LdG} and E_{OF} enables us to compare the two models and to introduce the notion of discrete orientable and non-orientable stable configurations. In Figure 2 we depict a non-orientable line field in G and a possible discrete vector field n_h such that $Q_h(z) = n_h(z) \otimes n_h(z)$ for all nodes z. This discrete effect is reflected in the critical mesh-dependence of E_{OF}. The energies are $E_{LdG} \approx 0.9543$ and $E_{OF} \approx 13.7151$, thus, the jump in n_h contributes dramatically

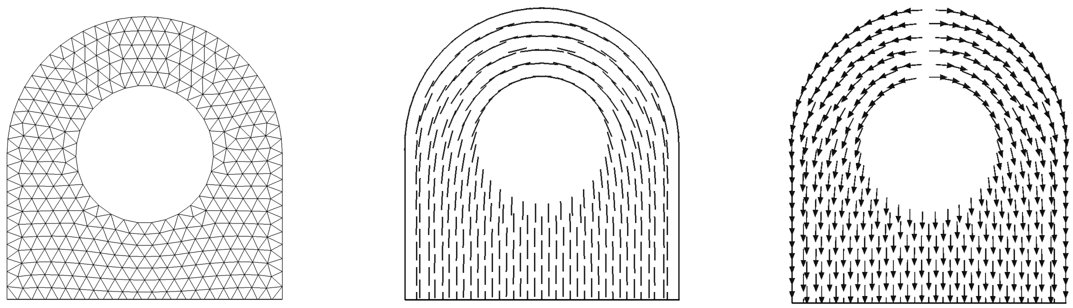

FIGURE 2. Discrete line fields and vector fields and triangulation of G (left). The line field Q_h (middle) and a possible discrete director field n_h that satisfies $Q_h(z) = n_h(z) \otimes n_h(z)$ at the nodes z. The vectors and lines at the nodes are scaled by the factor $1/5$. Note, that $E_{LdG}(Q_h) \approx 0.9543 \ll E_{OF}(n_h) \approx 13.7151$.

to the energy. The difference becomes even more dramatic when the mesh is refined reflecting the fact that there exists no continuous extension.

The outline of this work is as follows. In Section 2 we characterize the manifold $\mathbb{L}^2$ and derive Euler-Lagrange equations for E_{LdG}. In Section 3 we deduce a finite element discretization of E_{LdG} with pointwise constraints on the admissible functions. In Section 4 we propose an algorithm for the computation of Q harmonic line fields based on a gradient flow approach. Right after that we prove stability and convergence of the algorithm to a discrete Q harmonic line field in Section 5. Finally in Section 6 we execute some interesting experiments illustrating the performance of our algorithm. Furthermore, we numerically examine orientability issues discussed in [4] in two and three space dimensions.

2. Euler Lagrange equations for E_{LdG} and E_{OF}

We denote the tangent space of $\mathbb{L}^2$ at a given $Q_0 \in \mathbb{L}^2$ by $T_{Q_0}\mathbb{L}^2$ and for every tangent vector $V \in T_{Q_0}\mathbb{L}^2$ there exists a path $\gamma_0 : (-\delta, \delta) \to \mathbb{L}^2$ $(\delta > 0)$ satisfying $\gamma(0) = Q_0$ and $\frac{\mathrm{d}}{\mathrm{d}t}\Big|_{t=0}\gamma(t) = V$. The following lemma can be found in [4] and will help us to establish a complete characterization of $T_{Q_0}\mathbb{L}^2$. We include a sketch of the proof to give an idea of how to work with line fields.

Lemma 2.1 ([4], Lemma 3)**.** *If $-\infty < t_1 < t_2 < \infty$ and $Q : [t_1, t_2] \to \mathbb{L}^2$ is continuous then there exist exactly two continuous maps (liftings) $n^+, n^- : [t_1, t_2] \to \mathbb{S}^2$, so that $Q(t) = n^{\pm}(t) \otimes n^{\pm}(t)$ and $n^+ = -n^-$.*

Proof. Let $0 < \varepsilon < \sqrt{2}$. Given $n, \overline{m} \in \mathbb{S}^2$ with $|n \otimes n - \overline{m} \otimes \overline{m}| < \varepsilon$ we have that $2(1 - (n \cdot \overline{m})^2) = |n \otimes n - \overline{m} \otimes \overline{m}|^2 < \varepsilon^2$ and so

$$n \cdot \overline{m} \geq \sqrt{1 - \frac{\varepsilon^2}{2}} > 0 \qquad \text{or} \qquad n \cdot \overline{m} \leq -\sqrt{1 - \frac{\varepsilon^2}{2}} < 0.$$

Thus $n \otimes n = n^+ \otimes n^+ = n^- \otimes n^-$, where $n^+ \cdot \overline{m} > 0$ and $n^- = -n^+$ satisfies $n^- \cdot \overline{m} < 0$. Now let $Q(\tau) = n(\tau) \otimes n(\tau)$ be continuous on $[t_1, t_2]$. Then there exists $\delta > 0$ such that $|n(\tau) \otimes n(\tau) - n(\sigma) \otimes n(\sigma)| \leq \sqrt{2}$. for all $\sigma, \tau \in [t_1, t_2]$ with $|\sigma - \tau| \leq \delta$, and we may suppose that $t_2 - t_1 = M\delta$ for some integer $M \in \mathbb{N}$. First take $\overline{m} := n(t_1)$ and for each $\tau \in [t_1, t_1 + \delta]$ choose $n^+(\tau)$ as above so that $n^+(\tau) \otimes n^+(\tau) = n(\tau) \otimes n(\tau)$ and $n^+(\tau) \cdot \overline{m} > 0$. We claim that $n^+ : [t_1, t_1 + \delta] \to \mathbb{S}^2$ is continuous. Indeed, let $\sigma_j \to \sigma$ in $[t_1, t_1 + \delta]$ and suppose for contradiction that $n(\sigma_j) \not\to n(\sigma)$. Then since $n^+(\sigma_j) \otimes n^+(\sigma_j) \to n^+(\sigma) \otimes n^+(\sigma)$ there is a subsequence σ_{j_k} such that $n^+(\sigma_{j_k}) \to -n^+(\sigma)$. But then $-n^+(\sigma) \cdot \overline{m} \geq 0$ a contradiction which proves the claim. Repeating this procedure with $\overline{n} := n^+(t_1 + \delta)$ we obtain a continuous lifting $n^+ : [t_1, t_1 + 2\delta] \to \mathbb{S}^2$, and thus inductively a continuous lifting $n^+ : [t_1, t_2] \to \mathbb{S}^2$. Setting $n^- = -n^+$ gives a second continuous lifting. Again, by a standard continuity argument we see that there exist only two continuous liftings. $\square$

Let $n_0 \in \mathbb{S}^2$ satisfy $Q_0 = n_0 \otimes n_0$. According to Lemma 2.1, there exists for $\delta > 0$ a $\tilde{\gamma} : (-\delta, \delta) \to \mathbb{S}^2$ satisfying $\tilde{\gamma}(0) = n_0$ and define $\gamma|_{(-\delta,\delta)} = \tilde{\gamma} \otimes \tilde{\gamma}|_{(-\delta,\delta)}$. We define $\frac{\mathrm{d}}{\mathrm{d}t}\Big|_{t=0}\tilde{\gamma} := v \in T_{n_0}\mathbb{S}^2$ and obtain $V \in T_{Q_0}\mathbb{L}^2$

as

$$V = \frac{\mathrm{d}}{\mathrm{d}t}\Big|_{t=0}\gamma(t) = \frac{\mathrm{d}}{\mathrm{d}t}\Big|_{t=0}\tilde{\gamma}(t)\otimes\tilde{\gamma}(t) = n_0\otimes\frac{\mathrm{d}}{\mathrm{d}t}\Big|_{t=0}\tilde{\gamma}(t) + \frac{\mathrm{d}}{\mathrm{d}t}\Big|_{t=0}\tilde{\gamma}(t)\otimes n_0 = n_0\otimes v + v\otimes n_0.$$

This means, that there is a one-to-one correspondence between the tangent space $T_{Q_0}\mathbb{L}^2$ and $T_{n_0}\mathbb{S}^2$.

Let $\partial\Omega = \Gamma_{nor}\cup\Gamma_{tan}\cup\Gamma_N$ be a partition of the boundary of Ω. For line fields and director fields we impose natural Neumann boundary conditions on Γ_N and the essential boundary conditions of homeotropic anchoring and planar anchoring on Γ_{nor} and Γ_{tan}, respectively:

	$Q = n^Q\otimes n^Q \in \mathbb{L}^2$	$n\in\mathbb{S}^2$
$x\in\Gamma_{tan}$	$n^Q(x)\,\vert\vert\,\nu_{\partial\Omega}(x)$	$n(x)\,\vert\vert\,\nu_{\partial\Omega}(x)$
$x\in\Gamma_{nor}$	$n^Q(x)\perp\nu_{\partial\Omega}(x)$	$n(x)\perp\nu_{\partial\Omega}(x)$

Admissible tensor and director fields for E_{LdG} and E_{OF} are

$\mathcal{A}_{LdG} := \{Q\in W^{1,2}(\Omega,\mathbb{R}^{3\times 3}) : Q\in\mathbb{L}^2$ a.e. in Ω, Q satisfies the boundary conditions on $\Gamma_{nor}\cup\Gamma_{tan}\}$, and

$$\mathcal{A}_{OF} := \{n\in W^{1,2}(\Omega,\mathbb{R}^3) : n\in\mathbb{S}^2 \text{ a.e. in } \Omega,\ n \text{ satisfies the boundary conditions on } \Gamma_{nor}\cup\Gamma_{tan}\}.$$

Stationary points of E_{LdG} in the set of admissible line fields satisfy the imposed boundary conditions and

$$(\nabla Q, \nabla V) = 0,$$

for all $V\in\mathcal{F}_{\mathbb{L}^2}[Q]$ given by

$$\mathcal{F}_{\mathbb{L}^2}[Q] := \{V\in C_0^\infty(\overline{\Omega}\setminus(\Gamma_{nor}\cup\Gamma_{tan}),\mathbb{R}^{3\times 3}) : V(x)\in T_{Q(x)}\mathbb{L}^2 \text{ for } x\in\Omega\}.$$

At least locally, there exists always a vector field n satisfying $Q = n^Q\otimes n^Q$ and therefore we can rewrite the Euler Lagrange equation as

$$(\nabla Q, \nabla(n^Q\otimes v + v\otimes n^Q)) = 0$$

for all $v\in\mathcal{F}_{\mathbb{S}^2}[n^Q]$ given by

$$\mathcal{F}_{\mathbb{S}^2}[n^Q] := \{v\in C_0^\infty(\overline{\Omega}\setminus(\Gamma_{nor}\cup\Gamma_{tan}),\mathbb{R}^3) : v(x)\in T_{n^Q(x)}\mathbb{S}^2 \text{ for } x\in\Omega\}.$$

Stationary points of E_{OF} in the set $\mathcal{A}_{OF}$ satisfy the imposed boundary conditions and the Euler Lagrange equations

$$(\nabla n, \nabla v) = 0$$

for all $v\mathcal{F}_{\mathbb{S}^2}[n]$. Clearly, it is only possible to consider E_{OF} if the boundary values are orientable in the sense that there exists an orientable line field realizing the boundary conditions.

3. Discrete setting

We let $\mathcal{T}_h$ be a regular triangulation into triangles ($d=2$) or tetrahedra ($d=3$) of maximal diameter $h>0$ in the sense of [9]. We denote by $\mathbb{V} = \mathbb{V}(\mathcal{T}_h)$ the space of all continuous functions on Ω that are affine on the elements in the triangulation $\mathcal{T}_h$ and we set $\mathbb{V}_{nor} = \mathbb{V}\cap\{v\in W^{1,2}(\Omega) : v|_{\Gamma_{nor}} = 0\}$. We call a triangulation $\mathcal{T}_h$ *weakly acute* if

$$K_{ij} := \int_\Omega \nabla\varphi_{a_i}\cdot\nabla\varphi_{a_j}\,\mathrm{d}x \le 0 \quad \text{for all } a_i\neq a_j\in\mathcal{N}, \tag{3.1}$$

where $\mathcal{N} = \{a_1,\ldots,a_N\}$ denotes the set of nodes in $\mathcal{T}_h$ and $(\varphi_a)_{a\in\mathcal{N}}$ is the standard nodal basis of $\mathbb{V}$. Note that if $d=2$ the triangulation $\mathcal{T}_h$ is weakly acute if the sum of every pair of angles opposite to an interior edge is bounded by π and if the angle opposite to every edge on the boundary is less than or equal to $\pi/2$. We denote by $\mathcal{I}_h : C^0(\Omega)\to\mathbb{V}$ the standard nodal interpolant and for a fixed time-step size $\tau>0$ let $t_j = j\tau$ for all $j\ge 0$.

3.1. **Monotonicity estimates.** We include a monotonicity estimate from [6] that is a discrete version of a corresponding statement in [2].

Lemma 3.1 (Monotonicity I). *Let $\mathcal{T}_h$ be weakly acute, and let $\tilde{n}_h \in \mathbb{V}^3$ be such that $|\tilde{n}_h(a)| \geq 1$ for all $a \in \mathcal{N}$, and define $n_h \in \mathbb{V}^3$ by setting $n_h(a) = \tilde{n}_h(a)/|\tilde{n}_h(a)|$ for all $a \in \mathcal{N}$. Then*

$$\|\nabla n_h\| \leq \|\nabla \tilde{n}_h\|. \tag{3.2}$$

Proof. Let $(\varphi_{a_i})_{a_i \in \mathcal{N}}$ denote the nodal basis of $\mathbb{V}$. Besides (3.1), the symmetric matrix $(K_{ij})_{i,j=1}^N$ satisfies $\sum_{j=1}^N K_{ij} = 0$ owing to $\sum_{j=1}^N \varphi_{a_j} = 1$. We observe the relations

$$\begin{aligned}
||\nabla n_h||^2 &= \sum_{i,j=1}^N K_{ij} n_h(a_i) \cdot n_h(a_j) \\
&= \frac{1}{2}\sum_{i,j=1}^N K_{ij} n_h(a_i) \cdot \big(n_h(a_j) - n_h(a_i)\big) + \frac{1}{2}\sum_{i,j=1}^N K_{ij} n_h(a_j) \cdot \big(n_h(a_i) - n_h(a_j)\big) \\
&= -\frac{1}{2}\sum_{i,j=1}^N K_{ij} \big|n_h(a_i) - n_h(a_j)\big|^2.
\end{aligned}$$

The assertion is proved if $|n_h(a_i) - n_h(a_j)|^2 \leq |\tilde{n}_h(a_i) - \tilde{n}_h(a_j)|^2$ for all $i, j = 1, \cdots, N$. Hence, it suffices to show $\big|\frac{a}{|a|} - \frac{b}{|b|}\big| \leq \big|a - b\big|$, for $a, b \in \mathbb{R}^3$ with $|a|, |b| \geq 1$. This follows from the Lipschitz continuity with constant 1 of the map $\pi_{\mathbb{S}^2} : \{x \in \mathbb{R}^3 : |x| \geq 1\} \to \mathbb{S}^2$, $x \mapsto x/|x|$. □

Before we turn to the characterization of discrete harmonic director fields and Q harmonic line fields we state another monotonicity estimate result which is an adoption from the previous argument to the finite element space of functions that have nodal values in $\mathbb{L}^2$. The result is a consequence of the following auxiliary estimate.

Lemma 3.2 (Tensor Estimate). *Let $\tilde{v}, \tilde{w} \in \mathbb{R}^3$ such that $|\tilde{v}|, |\tilde{w}| \geq 1$. Set $v = \tilde{v}/|\tilde{v}|$ and $w = \tilde{w}/|\tilde{w}|$, then*

$$1 - (v \otimes v) : (w \otimes w) \leq \frac{1}{2}\Big|\tilde{v} \otimes \tilde{v} - \tilde{w} \otimes \tilde{w}\Big|^2, \tag{3.3}$$

where for $A, B \in \mathbb{R}^3$ $A : B = \operatorname{tr}(A^T B)$ and $\operatorname{tr} : \mathbb{R}^{3\times 3} \to \mathbb{R}$ is the usual trace of a square matrix.

Proof. We deduce

$$1 - (v \otimes v) : (w \otimes w) = 1 - (v \cdot w)^2 = (1 - v \cdot w)(1 + v \cdot w) = \frac{1}{4}|v - w|^2 |v + w|^2.$$

Where we incorporated the identity $1 \pm v \cdot w = \frac{1}{2}|v|^2 + \frac{1}{2}|w|^2 \pm v \cdot w = \frac{1}{2}|v \pm w|^2$ and the fact that

$$(v \otimes v) : (w \otimes w) = \sum_{k,\ell} v_k v_\ell w_k w_\ell = \sum_k v_k w_k \sum_\ell v_\ell w_\ell = (v \cdot w)^2.$$

Since $\pi_{\mathbb{S}^2}$ is point symmetric with respect to the origin and Lipschitz continuous on $\mathbb{R}^3 \setminus B_1(0)$ with Lipschitz constant one we deduce that

$$|v \pm w| = \Big|\frac{\tilde{v}}{|\tilde{v}|} \pm \frac{\tilde{w}}{|\tilde{w}|}\Big| \leq |\tilde{v} \pm \tilde{w}|.$$

This yields

$$\begin{aligned}
1 - (v \otimes v) : (w \otimes w) \leq \frac{1}{4}|\tilde{v} - \tilde{w}|^2 |\tilde{v} + \tilde{w}|^2 &= \frac{1}{4}\Big(|\tilde{v}|^2 + |\tilde{w}|^2 - 2\tilde{v} \cdot \tilde{w}\Big)\Big(|\tilde{v}|^2 + |\tilde{w}|^2 + 2\tilde{v} \cdot \tilde{w}\Big) \\
&= \frac{1}{4}\Big[\big(|\tilde{v}|^2 + |\tilde{w}|^2\big)^2 - 4(\tilde{v} \cdot \tilde{w})^2\Big] \\
&= \frac{1}{4}\Big[\big(|\tilde{v}|^4 - 2(\tilde{v} \cdot \tilde{w})^2 + |\tilde{w}|^4\big) + 2\left(|\tilde{v}|^2|\tilde{w}|^2 - (\tilde{v} \cdot \tilde{w})^2\right)\Big] \\
&\leq \frac{1}{2}\left(|\tilde{v}|^4 - 2(\tilde{v} \cdot \tilde{w})^2 + |\tilde{w}|^4\right) = \frac{1}{2}\Big|\tilde{v} \otimes \tilde{v} - \tilde{w} \otimes \tilde{w}\Big|^2,
\end{aligned}$$

where we used Young's inequality $2|\tilde{v}|^2|\tilde{w}|^2 \leq |\tilde{v}|^4 + |\tilde{w}|^4$ and the identity $|\tilde{v}|^4 = |\tilde{v} \otimes \tilde{v}|^2$. □

Lemma 3.3 (Monotonicity II)**.** *Let $\mathcal{T}_h$ be weakly acute, and let $\tilde{n}_h \in [\mathbb{V}]^3$ be such that $|\tilde{n}_h(a)| \geq 1$ for all $a \in \mathcal{N}$, and define $n_h \in [\mathbb{V}]^3$ by setting $n_h(a) = \tilde{n}_h(a)/|\tilde{n}_h(a)|$ for all $a \in \mathcal{N}$. Furthermore we define $\widetilde{Q}_h, Q_h \in [\mathbb{V}]^{3\times 3}$ by setting*

$$\widetilde{Q}_h(a) := \tilde{n}_h(a) \otimes \tilde{n}_h(a) \quad \textit{and} \quad Q_h(a) := \frac{\tilde{n}_h(a)}{|\tilde{n}_h(a)|} \otimes \frac{\tilde{n}_h(a)}{|\tilde{n}_h(a)|} \quad \textit{for all } a \in \mathcal{N}.$$

Then

$$\|\nabla Q_h\| \leq \|\nabla \widetilde{Q}_h\| \tag{3.4}$$

Proof. We start the proof with the same arguments as in Lemma 3.1 which yield

$$\begin{aligned}
\|\nabla Q_h\|^2 &= -\frac{1}{2}\sum_{i,j}^{N} K_{ij}|Q_h(a_i) - Q_h(a_j)|^2 \\
&= -\frac{1}{2}\sum_{i,j}^{N} K_{ij}\left(|Q_h(a_i)|^2 - 2Q_h(a_i) : Q_h(a_j) + |Q_h(a_j)|^2\right) \\
&= -\sum_{i,j}^{N} K_{ij}\left(1 - Q_h(a_i) : Q_h(a_j)\right).
\end{aligned}$$

For $i, j \in \{1, \ldots, N\}$ arbitrary we incorporate the estimate (3.3) from Lemma 3.2 with $\tilde{v} := \tilde{n}_h(a_i)$, $\tilde{w} := \tilde{n}_h(a_j)$, $v = \tilde{v}/|\tilde{v}|$ and $w = \tilde{w}/|\tilde{w}|$ and arrive at

$$1 - Q_h(a_i) : Q_h(a_j) \leq \frac{1}{2}|\widetilde{Q}_h(a_i) - \widetilde{Q}_h(a_j)|^2.$$

We conclude

$$||\nabla Q_h||^2 = -\sum_{ij} K_{ij}(1 - Q_h(a_i) : Q_h(a_j)) \leq -\frac{1}{2}\sum_{ij} K_{ij}|\widetilde{Q}_h(a_i) - \widetilde{Q}_h(a_j)|^2 = ||\nabla \widetilde{Q}_h||^2,$$

which proves the lemma. ◻

3.2. **Euler Lagrange equation in the discrete setting.** For the discrete version of the boundary conditions we assume that all nodes on the boundary of Ω lie either in Γ_N, Γ_{tan} or Γ_{nor}. For discrete line and director fields we impose natural Neumann boundary conditions on Γ_N and the discrete essential boundary conditions of homeotropic anchoring and planar anchoring on Γ_{nor} and Γ_{tan}, respectively:

	$Q_h(z) = n_h^Q(z) \otimes n_h^Q(z) \in \mathbb{L}^2$ for all $z \in \mathcal{N}_h$	$n_h(z) \in \mathbb{S}^2$ for all $z \in \mathcal{N}_h$
$z \in \Gamma_{tan}$	$n_h^Q(z) \,\|\, \nu_{\partial\Omega}(z)$	$n_h(z) \,\|\, \nu_{\partial\Omega}(z)$
$z \in \Gamma_{nor}$	$n_h^Q(z) \perp \nu_{\partial\Omega}(z)$	$n_h(z) \perp \nu_{\partial\Omega}(z)$

Thus, we define the discrete admissible line fields and director fields for E_{LdG} and E_{OF}:

$\mathcal{A}^h_{LdG} := \{P_h \in [\mathbb{V}]^{3\times 3} : P_h(a) \in \mathbb{L}^2$ for all $a \in \mathcal{N},\ P_h$ satisfies the boundary conditions on $\Gamma_{nor} \cup \Gamma_{tan}\}$, and

$$\mathcal{A}^h_{OF} := \{v_h \in [\mathbb{V}]^3 : v_h(a) \in \mathbb{S}^2 \text{ for all } a \in \mathcal{N},\ v_h \text{ satisfies the boundary conditions on } \Gamma_{nor} \cup \Gamma_{tan}\}.$$

Definition 3.4. *(i) A map $Q_h \in \mathcal{A}^h_{LdG}$ is called a* discrete Q harmonic tensor field *into $\mathbb{L}^2$ subject to homeotropic anchoring, planar anchoring and Neumann boundary conditions if Q_h is stationary for E_{LdG} among all $P_h \in \mathcal{A}^h_{LdG}$.*
(ii) A vector field $n_h \in \mathcal{A}^h_{OF}$ is called a discrete harmonic director field *subject to homeotropic anchoring, planar anchoring and Neumann boundary conditions if n_h is stationary for E_{OF} among all $v_h \in \mathcal{A}^h_{OF}$.*

Given $n_h \in \mathcal{A}^h_{OF}$ we define the space of tangential updates with respect to the sphere by

$$\mathcal{F}_{\mathbb{S}^2}[n_h] = \left\{r_h \in [\mathbb{V}_{nor}]^3 : r_h(a) \cdot n_h(a) = 0 \ \text{ for all } a \in \mathcal{N}, \text{ and } r_h(a) \cdot \nu_{\partial\Omega}(a) = 0 \ \text{ for all } a \in \mathcal{N} \cap \Gamma_{tan}\right\}. \tag{3.5}$$

For computations with line fields we define the space of tangential updates for a given $Q_h \in \mathcal{A}^h_{LdG}$ as

$$\mathcal{F}_{\mathbb{L}^2}[Q_h] = \big\{ R_h \in [\mathbb{V}_{nor}]^{3\times 3} : R_h = \mathcal{I}_h[r_h \otimes n_h^Q + n_h^Q \otimes r_h] \text{ for } r_h \in \mathcal{F}_{\mathbb{S}^2}[n_h^Q] \big\}, \tag{3.6}$$

where $n_h^Q \in [\mathbb{V}]^3$ satisfies $|n_h^Q(a)| = 1$ and $Q_h(a) = n_h^Q(a) \otimes n_h^Q(a)$ for all $a \in \mathcal{N}$. The following proposition is a variation of Lemma 3.1.4 from [5].

Proposition 3.5. *(1) A tensor field $Q_h \in \mathcal{A}^h_{LdG}$ is a discrete Q harmonic tensor field into $\mathbb{L}^2$ according to Definition 3.4 if and only if there holds*

$$(\nabla Q_h, \nabla V_h) = 0 \tag{3.7}$$

for all $V_h \in \mathcal{F}_{\mathbb{L}^2}[Q_h]$.

(2) A vector field $n_h \in \mathcal{A}^h_{OF}$ is a discrete harmonic director field according to Definition 3.4 if and only if there holds

$$(\nabla n_h, \nabla v_h) = 0 \tag{3.8}$$

for all $v_h \in \mathcal{F}_{\mathbb{S}^2}[n_h]$.

Proof. For the proof of (1) we note that a variation of Q_h can be given by $\mathcal{I}_h \pi_{\mathbb{L}^2}(Q_h + tP_h)$ for $t > 0$ small enough and $P_h \in [\mathbb{V}_{nor}]^{3\times 3}$. Then

$$\mathcal{I}_h \pi_{\mathbb{L}^2}(Q_h + tP_h)(a) = Q_h(a) + tD\pi_{\mathbb{L}^2}(Q_h(a))P_h(a) + o(t)$$

for all $a \in \mathcal{N}$. If $P_h \in \mathcal{F}_{\mathbb{L}^2}[Q_h]$ then $D\pi_{\mathbb{L}^2}(Q_h(a))P_h(a) = P_h(a)$ for all $a \in \mathcal{N}$ and we obtain that

$$\mathcal{I}_h \pi_{\mathbb{L}^2}(Q_h + tP_h) = Q_h + tP_h + o(t).$$

Thus, (3.7) follows by computing

$$0 = \lim_{t\to 0} t^{-1} \left(E_{LdG}(\mathcal{I}_h \pi_{\mathbb{L}^2}(Q_h + tP_h)) - E_{LdG}(Q_h) \right) = \left(\nabla Q_h, \nabla P_h \right).$$

The proof of (2) follows analogously. $\square$

4. Iterative Algorithms

We compute stationary points of E_{OF} and E_{LdG} via iterative algorithms that are motivated by the corresponding H^1 gradient flows. The continuous H^1 gradient flow for harmonic maps into a submanifold $\Sigma \subset \mathbb{R}^n$ subject to Dirichlet conditions on Γ_D seeks a function $V : (0,\infty) \times \Omega \to \Sigma$ satisfying $V(0,\cdot) = V_0$, $V(t,\cdot)|_{\Gamma_D} = V_D$ and

$$(\nabla \partial_t V, \nabla P) + (\nabla V, \nabla P) = 0 \tag{4.1}$$

for almost every $t \in (0,\infty)$ and all $P \in W^{1,2}_D(\Omega, \mathbb{R}^n)$ such that $P(x) \in T_{V(x)}\Sigma$ for almost every $x \in \Omega$.

4.1. Fully discrete algorithm for discrete harmonic director fields.

For the computation of discrete harmonic director fields a semi-implicit discretization of (4.1) yields the following algorithm. Well-posedness, unconditional stability for weakly acute triangulations, termination and convergence of the algorithm can be found in [6].

Input Triangulation $\mathcal{T}_h$, stopping criterion $\varepsilon > 0$, time-step size $\tau > 0$ and $n_h^0 \in \mathcal{A}^h_{OF}$. Set $i = 0$.

(1) Compute $w_h^i \in \mathcal{F}_{\mathbb{S}^2}[n_h^i]$ such that

$$\Big(\nabla w_h^i, \nabla v_h\Big) + \Big(\nabla (n_h^i + \tau w_h^i), \nabla v_h\Big) = 0$$

for all $v_h \in \mathcal{F}_{\mathbb{S}^2}[n_h^i]$.

(2) Set

$$n_h^{i+1}(a) := \frac{n_h^i(a) + \tau w_h^i(a)}{|n_h^i(a) + \tau w_h^i(a)|},$$

for all $a \in \mathcal{N}$.

(3) Stop, if $||\nabla w_h^i||_{L^2} < \varepsilon$.

(4) Set $i = i + 1$ and go to (1).

Output: $n_h^* := n_h^i$.

Remark 4.1. (i) For $\mathrm{d}_t n_h^i := w_h^i$ and $\tilde{n}_h^{i+1} := n_h^i + \tau \mathrm{d}_t n_h^i$ the equation in Step (1) reads

$$(\nabla \mathrm{d}_t n_h^i, \nabla v_h) + (\nabla \tilde{n}_h^{i+1}, \nabla v_h) = 0$$

which is a discrete version of (4.1).
(ii) As it was already discussed in [7, 16] the same algorithm without Step 2 yields for the output n_h^*

$$||\mathcal{I}_h[|n_h^*|^2 - 1]||_{L^1} \leq C\tau E_{OF}(n_h^0).$$

Thus, for $\tau > 0$ small enough the projection step can be skipped and the violation of the constraint at the nodes is controlled by the time-step size τ.

4.2. **Fully discrete algorithm for discrete Q harmonic tensor fields.** For the computation of discrete Q harmonic tensor fields we propose the following algorithm which is a discretization of a variation of the H^1 gradient flow. Locally, we have that $Q = n^Q \otimes n^Q$ and $\partial_t Q = \partial_t n^Q \otimes n^Q + n^Q \otimes \partial_t n^Q$ as well as the relation $V = n^Q \otimes v + v \otimes n^Q$ for $V \in \mathcal{F}_{\mathbb{L}^2}[Q]$ and some $v \in \mathcal{F}_{\mathbb{S}^2}[n^Q]$. We employ the modified H^1 gradient flow as

$$(\nabla \partial_t n^Q, \nabla v) + \lambda(\nabla \partial_t Q, \nabla V) + (\nabla Q, \nabla V) = 0,$$

with a discretization parameter $\lambda > 0$ that coincides with the time-step size. In Section 5 we will provide proofs of stability, termination and convergence of the algorithm to a discrete Q harmonic tensor field.

Input Triangulation $\mathcal{T}_h$, stopping criterion $\varepsilon > 0$, time-step size $\tau > 0$ and $Q_h^0 \in \mathcal{A}_{LdG}^h$. Set $i := 0$.

(1) Compute $w_h^i \in \mathcal{F}_{\mathbb{S}^2}[n_h^{Q,i}]$ such that

$$\Big(\nabla w_h^i, \nabla v_h\Big) + \Big(\nabla(Q_h^i + \tau \mathcal{I}_h[n_h^{Q,i} \otimes w_h^i + w_h^i \otimes n_h^{Q,i}]), \nabla \mathcal{I}_h[n_h^{Q,i} \otimes v_h + v_h \otimes n_h^{Q,i}]\Big) = 0,$$

for all $v_h \in \mathcal{F}_{\mathbb{S}^2}[n_h^{Q,i}]$.

(2) Set

$$Q_h^{i+1}(a) := \frac{n_h^{Q,i}(a) + \tau w_h^i(a)}{|n_h^{Q,i}(a) + \tau w_h^i(a)|} \otimes \frac{n_h^{Q,i}(a) + \tau w_h^i(a)}{|n_h^{Q,i}(a) + \tau w_h^i(a)|},$$

for all $a \in \mathcal{N}$.

(3) Stop, if $||\nabla w_h^i||_{L^2} < \varepsilon$.

(4) Set $i = i + 1$ and go to (1).

Output: $Q_h^* = Q_h^i$.

5. Analysis of the algorithms and Q harmonic tensor fields

In the first part of this section we analyze the proposed algorithm for the computation of Q harmonic tensor fields. Related results for the H^1 gradient flow for director fields can be found in [6]. Furthermore, we discuss a weak compactness result for Q harmonic tensor fields on a continuous level which provides the basis for a convergence analysis of the discrete approximations. We refer to [5] for a corresponding analysis in the case of discrete harmonic director fields.

5.1. **Stability and convergence of the tensor field algorithm.** We start our analysis by showing well-posedness of the algorithm. A stability result enables us to show termination of the algorithm and convergence to discrete Q harmonic tensor field.

Lemma 5.1 (Well-posedness). *Given $Q_h \in [\mathbb{V}]^{3\times 3}$ satisfying $Q_h(a) \in \mathbb{L}^2$ for all $a \in \mathcal{N}$ there exists $w_h \in \mathcal{F}_{\mathbb{S}^2}[n_h^Q]$ satisfying*

$$\Big(\nabla w_h, \nabla v_h\Big) + \Big(\nabla(Q_h + \tau \mathcal{I}_h[n_h^Q \otimes w_h + w_h \otimes n_h^Q]), \nabla \mathcal{I}_h[n_h^Q \otimes v_h + v_h \otimes n_h^Q]\Big) = 0 \tag{5.1}$$

for all $v_h \in \mathcal{F}_{\mathbb{S}^2}[n_h^Q]$. Moreover we have the following estimate

$$\tau \|\nabla w_h\|^2 \leq E_{LdG}(Q_h). \tag{5.2}$$

Proof. We set

$$T := \Big\{ v_h \in [\mathbb{V}_{nor}]^3 \,:\, v_h(a) \in T_{n_h^Q(a)}\mathbb{S}^2 \text{ for all } a \in \mathcal{N} \Big\}$$

and note that T is a subspace of $[\mathbb{V}_{nor}]^3$. The bilinear form $A_Q : T \times T \to \mathbb{R}$, defined through

$$(w_h, v_h) \quad \mapsto \quad \Big(\nabla w_h, \nabla v_h\Big) + \Big(\nabla \mathcal{I}_h[n_h^Q \otimes w_h + w_h \otimes n_h^Q], \nabla \mathcal{I}_h[n_h^Q \otimes v_h + v_h \otimes n_h^Q]\Big)$$

fulfills the requirements of the Lax-Milgram Lemma. For the unique solution w_h of (5.1) we obtain by chosing $v_h = \tau w_h$ that

$$\begin{aligned}\tau\|\nabla w_h\|^2 + \tau^2\|\nabla \mathcal{I}_h[n_h^Q \otimes w_h + w_h \otimes n_h^Q]\|^2 &= -\tau\Big(\nabla Q_h, \nabla \mathcal{I}_h[n_h^Q \otimes w_h + w_h \otimes n_h^Q]\Big)\\ &\leq \frac{1}{4}\|\nabla Q_h\|^2 + \tau^2\|\nabla \mathcal{I}_h[n_h^Q \otimes w_h + w_h \otimes n_h^Q]\|^2,\end{aligned}$$

which is the asserted estimate. □

Lemma 5.2 (Stability)**.** *Assume that $\mathcal{T}_h$ is weakly acute. Given $Q_h^0 \in \mathcal{A}_{LdG}^h$ let $(Q_h^i)_{0\leq i\leq J} \subset \mathcal{A}_{LdG}^h$ be the sequence of tensor fields computed in our Q tensor field algorithm and let*

$$C' := 1 - CC_0^{1/2}\tau h^{1-d/2}(\log h_{min}^{-1}) - CC_0\tau^3 h^{2-d}(\log h_{min}^{-1})^2,$$

where $C_0 := E_{LdG}(Q_h^0)$, $h_{min}^2 := \min_{T\in\mathcal{T}_h}\text{diam}T$ and the constant $C > 0$ depends on the geometry of the mesh but is independent of the mesh-size $h > 0$. If the time-step size $\tau > 0$ is small enough, so that $C' > 0$ then for all $J \geq 1$

$$E_{LdG}(Q_h^{J+1}) + C'(\tau/2)\sum_{i=0}^{J}\|\nabla w_h^i\|^2 \leq E_{LdG}(Q_h^0),$$

and the Q-field algorithm terminates within a finite number of iterations.

Proof. We recall that $Q_h^i = \mathcal{I}_h[n_h^{Q,i} \otimes n_h^{Q,i}]$ and

$$Q_h^{i+1}(a) = \frac{n_h^{Q,i}(a) + \tau w_h^i(a)}{|n_h^{Q,i}(a) + \tau w_h^i(a)|} \otimes \frac{n_h^{Q,i}(a) + \tau w_h^i(a)}{|n_h^{Q,i}(a) + \tau w_h^i(a)|},$$

for all $a \in \mathcal{N}$. We set $\widetilde{Q}_h^{i+1} := Q_h^i + \tau\mathcal{I}_h[w_h^i \otimes n_h^{Q,i} + n_h^{Q,i} \otimes w_h^i]$ and $\widetilde{\widetilde{Q}}_h^{i+1} := \mathcal{I}_h[(n_h^{Q,i} + \tau w_h^i) \otimes (n_h^{Q,i} + \tau w_h^i)] = \widetilde{Q}_h^{i+1} + \tau^2\mathcal{I}_h[w_h^i \otimes w_h^i]$. Furthermore, we know that according to Lemma 3.3 $E_{LdG}(\widetilde{\widetilde{Q}}_h^{i+1}) \geq E_{LdG}(Q_h^{i+1})$, since $\mathcal{T}_h$ is weakly acute. In Step 1 of the algorithm we compute $w_h^i \in \mathcal{F}_{\mathbb{S}^2}[n_h^{Q,i}]$ satisfying

$$(\nabla w_h^i, \nabla v_h) + (\nabla \widetilde{Q}_h^i, \nabla \mathcal{I}_h[v_h \otimes n_h^{Q,i} + n_h^{Q,i} \otimes v_h]) = 0,$$

for all $v_h \in \mathcal{F}_{\mathbb{S}^2}[n_h^{Q,i}]$. We test the equation with $v_h = \tau w_h^i$ and obtain

$$\tau\|\nabla w_h^i\|^2 + (\nabla \widetilde{Q}_h^{i+1}, \nabla(\widetilde{Q}_h^{i+1} - Q_h^i)) = 0.$$

Upon using the binomial identity $2a(a-b) = (a-b)^2 + a^2 - b^2$ we infer that

$$\tau\|\nabla w_h^i\|^2 + 2(E_{LdG}(\widetilde{Q}_h^{i+1}) - E_{LdG}(Q_h^i)) + (\tau^2/2)\|\nabla \mathcal{I}_h[w_h^i \otimes n_h^{Q,i} + n_h^{Q,i} \otimes w_h^i]\|^2 = 0.$$

The monotonicity estimate for line fields together with the identity

$$E_{LdG}(\widetilde{\widetilde{Q}}_h^{i+1}) = E_{LdG}(\widetilde{Q}_h^{i+1}) + (\tau^2/2)(\nabla \widetilde{Q}_h^{i+1}, \nabla \mathcal{I}_h[w_h^i \otimes w_h^i]) + \tau^4 E_{LdG}(\mathcal{I}_h[w_h^i \otimes w_h^i])$$

yields

$$\begin{aligned}\tau\|\nabla w_h^i\|^2 + 2(E_{LdG}(Q_h^{i+1}) - E_{LdG}(Q_h^i)) + (\tau^2/2)\|\nabla \mathcal{I}_h[w_h^i \otimes n_h^{Q,i} + n_h^{Q,i} \otimes w_h^i]\|^2&\\ - \tau^2(\nabla \widetilde{Q}_h^{i+1}, \nabla \mathcal{I}_h[w_h^i \otimes w_h^i]) - 2\tau^4 E_{LdG}(\mathcal{I}_h[w_h^i \otimes w_h^i]) &\leq 0.\end{aligned}$$

To bound the first negative term we employ the representation of $\widetilde{Q}_h^{i+1}$ and Young's inequality

$$\begin{aligned}\tau^2(\nabla\widetilde{Q}_h^{i+1},\nabla\mathcal{I}_h[w_h^i\otimes w_h^i]) &= \tau^2(\nabla(Q_h^i+\tau\mathcal{I}_h[w_h^i\otimes n_h^{Q,i}+n_h^{Q,i}\otimes w_h^i]),\nabla\mathcal{I}_h[w_h^i\otimes w_h^i])\\ &\le 2\tau^2(E_{LdG}(Q_h^i))^{1/2}\|\nabla\mathcal{I}_h[w_h^i\otimes w_h^i]\|+2\tau^4E_{LdG}(\mathcal{I}_h[w_h^i\otimes w_h^i])\\ &\quad+(\tau^2/2)\|\nabla\mathcal{I}_h[w_h^i\otimes n_h^{Q,i}+n_h^{Q,i}\otimes w_h^i]\|^2.\end{aligned}$$

Thus, we arrive at

$$\begin{aligned}(5.3)\quad \tau\|\nabla w_h^i\|^2+2(E_{LdG}(Q_h^{i+1})-E_{LdG}(Q_h^i))\\ -2\tau^2(E_{LdG}(Q_h^i))^{1/2}\|\nabla\mathcal{I}_h[w_h^i\otimes w_h^i]\|-4\tau^4E_{LdG}(\mathcal{I}_h[w_h^i\otimes w_h^i])\le 0.\end{aligned}$$

We argue by induction and assume that $E_{LdG}(Q_h^j)\le C_0$ for $j=0,\dots,i$. A discrete norm equivalence on every triangle $T\in\mathcal{T}_h$ shows that

$$\|\nabla\mathcal{I}_h[w_h^i\otimes w_h^i]\|_{L^2(T)}\le C\|\nabla(w_h^i\otimes w_h^i)\|_{L^2(T)}\le 2C\|w_h^i\|_{L^\infty(T)}\|\nabla w_h^i\|_{L^2(T)}.$$

We incorporate the inverse estimate $\|w_h^i\|_{L^\infty(T)}\le Ch_T^{1-d/2}\log h_T^{-1}\|\nabla w_h^i\|_{L^2(T)}$, cf., e.g., [9], and sum over all $T\in\mathcal{T}_h$ to arrive at

$$\|\nabla\mathcal{I}_h[w_h^i\otimes w_h^i]\|\le Ch_{min}^{1-d/2}\log h_{min}^{-1}\|\nabla w_h^i\|^2.$$

Furthermore, if we incorporate (5.2) and the induction hypotheses we obtain the following bound

$$E_{LdG}(\mathcal{I}_h[w_h^i\otimes w_h^i])\le Ch_{min}^{2-d}(\log h_{min}^{-1})^2\|\nabla w_h^i\|^4\le CC_0\tau^{-1}h_{min}^{2-d}(\log h_{min}^{-1})^2\|\nabla w_h^i\|^2.$$

We use the derived bounds in (5.3) and deduce that

$$\tau(1-CC_0^{1/2}\tau h_{min}^{1-d/2}\log h_{min}^{-1}-CC_0\tau^2h_{min}^{2-d}(\log h_{min}^{-1})^2)\|\nabla w_h^i\|^2+2(E_{LdG}(Q_h^{i+1})-E_{LdG}(Q_h^i))\le 0.$$

Upon choosing $\tau>0$ small enough so that

$$C':=1-CC_0^{1/2}\tau h_{min}^{1-d/2}\log h_{min}^{-1}-CC_0\tau^2h_{min}^{2-d}(\log h_{min}^{-1})^2>0,$$

we obtain the local energy inequality

$$C'\tau\|\nabla w_h^i\|^2+2(E_{LdG}(Q_h^{i+1})-E_{LdG}(Q_h^i))\le 0.$$

Therefore, $E_{LdG}(Q_h^{i+1})\le E_{LdG}(Q_h^i)\le C_0$ and this allows us to proceed by induction. Summing over i from 0 to J yields

$$E_{LdG}(Q_h^{J+1})+C'(\tau/2)\sum_{i=0}^{J}\|\nabla w_h^i\|^2\le E_{LdG}(Q_h^0).$$

$\square$

Theorem 5.3 (Termination and convergence to a discrete Q harmonic tensor field)**.** *Suppose that the conditions of Lemma 5.1 and Lemma 5.2 are satisfied. Then the tensor field algorithm terminates within a finite number of iterations and the output $Q_h^*\in\mathcal{A}_{LdG}^h$ satisfies*

$$\left(\nabla Q_h^*,\nabla\mathcal{I}_h[n_h^{Q,*}\otimes v_h+v_h\otimes n_h^{Q,*}]\right)=\mathcal{R}es(v_h)$$

for all $v_h\in\mathcal{F}_{\mathbb{S}^2}[n_h^{Q,*}]$, where the linear functional $\mathcal{R}es:\mathcal{F}_{\mathbb{S}^2}[n_h^{Q,*}]\to\mathbb{R}$ satisfies $|\mathcal{R}es(v_h)|\le\varepsilon\|\nabla v_h\|^2$ for all $v_h\in\mathcal{F}_{\mathbb{S}^2}[n_h^{Q,*}]$. For a sequence $(\varepsilon_J)_{J\in\mathbb{N}}$ of positive numbers such that $\varepsilon_J\to 0$ as $J\to\infty$, every accumulation point of the corresponding bounded sequence of outputs $(Q_h^{*,J})_{J\in\mathbb{N}}\subset\mathcal{A}_{LdG}^h$ of the algorithm is a discrete Q harmonic line field according to Definition 3.4.

Proof. The proof is a direct consequence of Theorem 3.2.7 from [5]. $\square$

5.2. **Weak compactness result for Q harmonic tensor fields.** For ease of presentation we assume homeotropic boundary conditions on the entire boundary and let $(Q_\ell)_\ell \subset W^{1,2}(\Omega;\mathbb{L}^2)$ be a bounded sequence of Q harmonic tensor fields. Then there exists $\pm n_\ell : \Omega \to \mathbb{S}^2$ satisfying $Q_\ell(x) = n_\ell(x) \otimes n_\ell(x)$ for almost every $x \in \Omega$. Note that, on every simply connected $\omega \subset \Omega$ we can chose $\pm n_\ell \in W^{1,2}(\omega, \mathbb{S}^2)$. Moreover, we have that

$$(\nabla Q_\ell, \nabla V) = 0$$

for all $V \in W_0^{1,2}(\Omega; \mathbb{R}^{3\times 3})$ satisfying $V(x) \in T_{Q_\ell(x)}\mathbb{L}^2$ for almost every $x \in \Omega$. We will show convergence on every simply connected $\omega \subset \Omega$. For this let $V \in W_0^{1,2}(\Omega; \mathbb{R}^{3\times 3})$ be such that $\mathrm{supp} V \subset \omega$ and $V(x) \in T_Q(x)\mathbb{L}^2$ for almost every $x \in \omega$. Thus, there exists $v \in W_0^{1,2}(\omega, \mathbb{R}^3)$ satisfying $v(x) \in T_{n_\ell(x)}\mathbb{S}^2$ for almost every $x \in \omega$ and $V = n_\ell \otimes v + v \otimes n_\ell$. Furthermore, we can rewrite $v = n_\ell \times \zeta$ for some function $\zeta \in W_0^{1,2}(\omega, \mathbb{R}^3)$ and the usual cross product $\times$. From the boundedness of $(Q_\ell)_\ell$ we infer that for (not relabeled) subsequences

$$Q_\ell \rightharpoonup Q \text{ in } W^{1,2}, \quad Q_\ell \to Q \text{ in } L^2 \quad \text{and} \quad Q_\ell \to Q \text{ pointwise almost everywhere } \Omega.$$

Since $Q_\ell = n_\ell \otimes n_\ell$ almost every, we know that $n_\ell^i n_\ell^j \to n^i n^j$ pointwise almost everywhere for $i, j = 1, \dots, 3$. We proceed

$$\begin{aligned}
(\nabla Q_\ell, \nabla V) &= (\nabla Q_\ell, \nabla(n_\ell \otimes v + v \otimes n_\ell)) \\
&= (\nabla Q_\ell, \nabla(n_\ell \otimes (n_\ell \times \zeta) + (n_\ell \times \zeta) \otimes n_\ell)) \\
&= \sum_{k=1}^d (\partial_k Q_\ell, \partial_k(n_\ell \otimes (n_\ell \times \zeta) + (n_\ell \times \zeta) \otimes n_\ell)) \\
&= \sum_{k=1}^d ((\partial_k n_\ell) \otimes n_\ell + n_\ell \otimes (\partial_k n_\ell), \partial_k(n_\ell \otimes (n_\ell \times \zeta) + (n_\ell \times \zeta) \otimes n_\ell)).
\end{aligned}$$

For $a, b, c, d \in \mathbb{R}^3$ we have that $(a \otimes b, c \otimes d) = (a^T d, b^T c)$. Since $n_\ell \perp \partial_k n_\ell$ for $k = 1, \dots, d$ and $n_\ell \perp n_\ell \times \zeta$ we see that terms of the form

$$(\partial_k n_\ell \otimes n_\ell, \partial_k n_\ell \otimes (n_\ell \times \zeta)) = ((\partial_k n_\ell)^T (n_\ell \times \zeta), n_\ell^T (\partial_k n_\ell))$$

vanish and we obtain the identity

$$\begin{aligned}
(\nabla Q_\ell, \nabla V) &= \sum_{k=1}^d ((\partial_k n_\ell) \otimes n_\ell + n_\ell \otimes (\partial_k n_\ell), n_\ell \otimes (n_\ell \times \partial_k \zeta) + (n_\ell \times \partial_k \zeta) \otimes n_\ell)) \\
&= \sum_{k=1}^d (\partial_k Q_\ell, n_\ell \otimes (n_\ell \times \partial_k \zeta) + (n_\ell \times \partial_k \zeta) \otimes n_\ell)).
\end{aligned}$$

The products $n_\ell \otimes (n_\ell \times \partial_k \zeta)$ and $(n_\ell \times \partial_k \zeta) \otimes n_\ell$ are quadratic in the components of n_ℓ and therefore we have that $n_\ell \otimes (n_\ell \times \partial_k \zeta) \to n \otimes (n \times \partial_k \zeta)$ pointwise almost everywhere in Ω. Since $|n_\ell| = 1$ and $\zeta \in L^\infty$ we have by Lebesgue's dominated convergence that $n_\ell \otimes (n_\ell \times \partial_k \zeta) \to n \otimes (n \times \partial_k \zeta)$ strongly in L^2. Together with the weak convergence of $\partial_k Q_\ell$ we infer that

$$0 = (\nabla Q_\ell, \nabla V) \longrightarrow \sum_{k=1}^d (\partial_k Q, n \otimes (n \times \partial_k \zeta) + (n \times \partial_k \zeta) \otimes n)) = (\nabla Q, \nabla(n \otimes (n \times \zeta) + (n \times \zeta) \otimes n)).$$

Since this holds for all ζ and the previous arguments are independent of $\omega \subset \Omega$ we have that Q is a harmonic line field.

6. Numerical experiments

6.1. **Extinction of Singularities.** We consider a liquid crystal cell $V = (-1, 1)^3 \subset \mathbb{R}^3$ with planar anchoring conditions. In this case defects at the boundary can be observed leading to so called *Schlieren textures*. There are different types of defects (disclinations) and to each type is assigned a number and a sign. Some of them may cancel out each other if they come into contact. We consider the upper boundary of V and

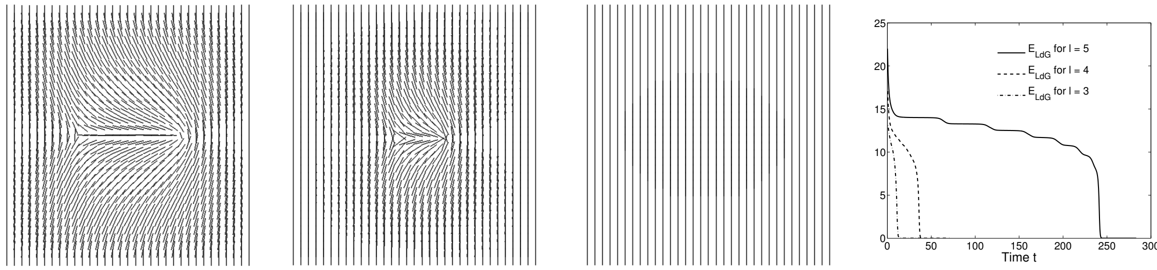

FIGURE 3. Annihilation of two opposite degree one-half singularities during the computation and an energy plot demonstrating the decay of energy for different mesh-sizes. The energy shows a strong decay when the attracting defects eventually annihilate.

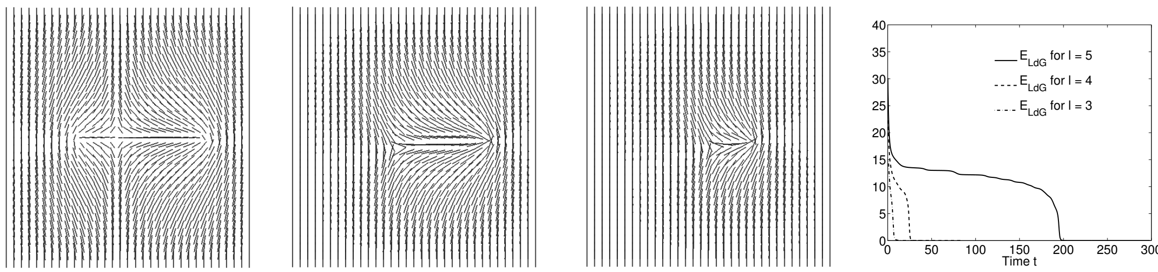

FIGURE 4. Extinction of three singularities during the computation and an energy plot demonstrating the decay of energy for different mesh-sizes: The nearby negative degree one and positive degree one-half singularities come together and result in a negative degree one-half singularity. Then, as in the first experiment an annihilation takes place when the remaining singularities meet. The energy shows strong decays when the annihilations take place.

simulate the annihilation of opposite degree one-half and degree one singularities in the iteration of the algorithm. The preference of the alignment parallel to the surface $\Omega = (-1,1)^2 \times \{1\}$ is modelled by the use of a Ginzburg-Landau penalty-term. Thus, we consider

$$E^{\varepsilon}_{LdG}(Q) = \frac{1}{2}\int_{\Omega} |\nabla Q|^2 \,\mathrm{d}x + \frac{1}{2\varepsilon^2}\int_{\Omega} |Q_{33}|^2 \,\mathrm{d}x.$$

Penalizing the out of plane component is physically consistent since the alignment parallel to Ω is favored but not forced. Mathematically this is crucial since the singularities in the plane have inifinite energy. Let $\mathcal{T}_{h,0}$ be a triangulation of Ω consisting of two triangles obtained by dividing $(-1,1)^2$ along the diagonal $x_1 = x_2$. The sequence of triangulations $\mathcal{T}_\ell$ is generated by ℓ uniform refinements of $\mathcal{T}_0$ with mesh-size $h_\ell = \sqrt{2}2^{-\ell}$. We use a time-step size $\tau = 5h$ and set $\varepsilon = 10^{-1}$. In our first experiment we examine the extinction of two opposite degree one-half singularities. We place a positive degree one-half singularity at $x_1 = 0.5$ and a negative degree one-half singularity at $x_1 = -0.5$. Boundary values are chosen to be $n_D = [0,1,0]^T$. The unique minimizer of E^{ε}_{LdG} is given by $u = [0,1,0]^T$. For the construction of such initial defect data we refer the reader to [8, 16]. In a second experiment we place a negative degree one singularity at $x_1 = 0$ and two positive degree one-half singularities at $x_1 = -0.3$ and $x_1 = 0.7$. As in the first experiment the boundary values are $n_D = [0,1,0]^T$. Snapshots of the evolution and decay of energy in the two examples can be seen in Figure 3 and Figure 4.

6.2. **Orientability versus non-orientability.** Let $D_1 := (-1.5,1.5) \times (-1,1)$, $D_2 := B_1([-1.5,0]^T) \cup B_1([1.5,0]^T)$, $D_3 := B_{1/2}([-1.5,0]^T) \cup B_{1/2}([1.5,0]^T)$ and $D := (D_1 \cup D_2) \setminus D_3$, see Figure 5. We use the DistMesh package [15] to generate quasi-uniform triangulations of D with arbitrary mesh-size. Thus, the quantities $h = 0.1, 0.075$ and $h = 0.05$ in Figure 5 are approximate values to the actual mesh-sizes according to the definition in Section 3. The twodimensional domain D was introduced in [4] to point out that there

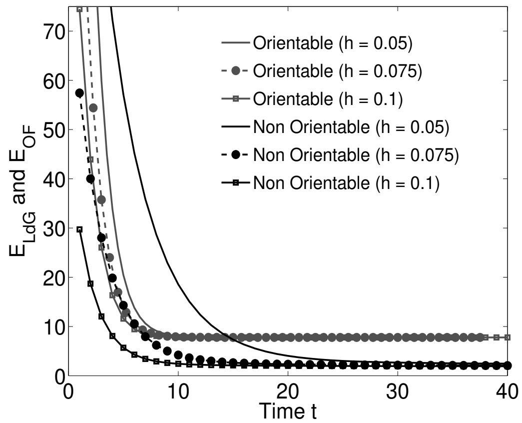

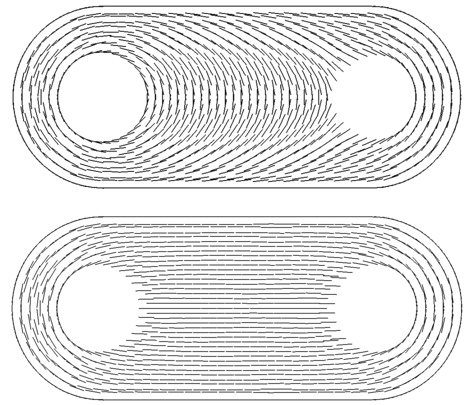

FIGURE 5. Energy decay for different mesh-sizes and final states for a triangulation of D with mesh size $h = 0.1$. The energy of the final state in the class of non-orientable line fields is strictly smaller than the energy in the class of orientable line fields. The classical Oseen-Frank theory would not detect the absolute minimum prefered by the liquid crystal.

exist settings in which the Q-tensor theory yields stable configurations that cannot be seen by the classical Oseen-Frank model. We impose tangential boundary conditions on the outer part of the boundary and Neumann conditions at the interior. Furthermore we consider the energy

$$E^{\varepsilon}_{LdG}(Q) = \frac{1}{2}\int_{\Omega} |\nabla Q|^2 \,\mathrm{d}x + \frac{1}{2\varepsilon^2}\int_{\Omega} |Q_{33}|^2 \,\mathrm{d}x,$$

which allows for an out-of-plane component and thereby for singularities in the interior as in Subsection 6.1. We compute stable configurations in the class of orientable and non-orientable line fields with our algorithms from Section 4, see Figure 5 and Figure 6. We observe for a sequence of triangulations with approximate mesh-sizes $h = 0.1, 0.075$ and $h = 0.05$ that the energies in the class of non-orientable line fields are strictly smaller than the energies in the class of orientable line fields. Thus, the classical Oseen-Frank theory fails to detect stable configurations of the liquid crystal with small energy.

6.3. **Torus experiments.** We investigate stable configurations of line fields on a vertically stretched torus $\mathbb{T}^2$ which can be parametrized by $X : (0, 2\pi)^2 \to \mathbb{R}^3$,

$$(\varphi, \theta) \mapsto \begin{bmatrix} (R + r\cos\theta)\cos\varphi \\ (R + r\cos\theta)\sin\varphi \\ 2.5r\sin\theta \end{bmatrix}$$

with $R > r > 0$, see Figure 7. Planar anchoring conditions are imposed everywhere on the surface and we compute the tangent vectors

$$\tau_1 := \frac{\partial_\varphi X}{|\partial_\varphi X|} \quad \text{and} \quad \tau_2 := \frac{\partial_\theta X}{|\partial_\varphi X|},$$

as well as the unit normal outer normal $\nu = \frac{\tau_1 \times \tau_2}{|\tau_1 \times \tau_2|}$. Let $\widetilde{\mathcal{T}}_0$ be a triangulation of $(0, 2\pi)^2$ consisting of two triangles obtained by dividing $(0, 2\pi)^2$ along the diagonal $x_1 = x_2$. The sequence of triangulations $\widetilde{\mathcal{T}}_\ell$ with mesh-size $\widetilde{h}_\ell = \sqrt{2}(2\pi)2^{-\ell}$ and nodes $\widetilde{\mathcal{N}}_\ell$ is generated by ℓ uniform refinements of $\widetilde{\mathcal{T}}_0$. We identify the following nodes

$$[0, \xi_{\widetilde{h}_\ell}]^T \;\longleftrightarrow\; [2\pi, \xi_{\widetilde{h}_\ell}]^T \quad \text{and} \quad [\xi_{\widetilde{h}_\ell}, 0]^T \;\longleftrightarrow\; [\xi_{\widetilde{h}_\ell}, 2\pi]^T$$

for $\xi_{\widetilde{h}_\ell} = 0, \widetilde{h}/\sqrt{2}, 2\widetilde{h}/\sqrt{2}, \ldots, 2\pi$. By this, we obtain a new triangulation $\mathcal{T}_\ell$ with a new set of nodes $\overline{\mathcal{N}}_\ell$ and define

$$\mathcal{N}_\ell = \Big\{ X(z) : \, z \in \overline{\mathcal{N}}_\ell \Big\}.$$

This results in a closed triangulated surface $\mathbb{T}^2_h$ approximating $\mathbb{T}^2$ with a new mesh size $h_\ell = ||DX||_{L^\infty}\widetilde{h}_\ell > 0$,

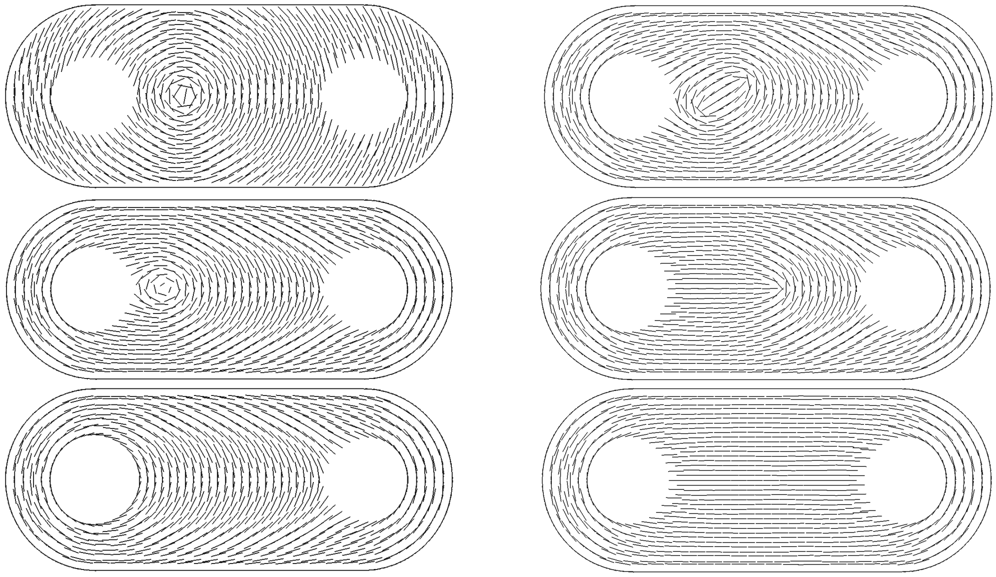

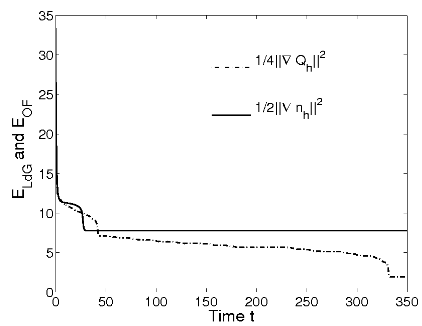

FIGURE 6. Snapshots of an evolution under the H^1 gradient flow and decay of energy for director fiels (left) and line fields (right): The initial line field Q_h^0 admits a positive degree one singularity at $x_1 = -0.5$, the holes are located at $x_1 = \pm 1.5$ and have a radius $r = 0.5$. In the orientable case the singularity moves into the hole on the right. In the non-orientable case the singularity splits into two positive degree one-half singularities that repulse from each other and vanish in the holes leading to a strictly smaller energy.

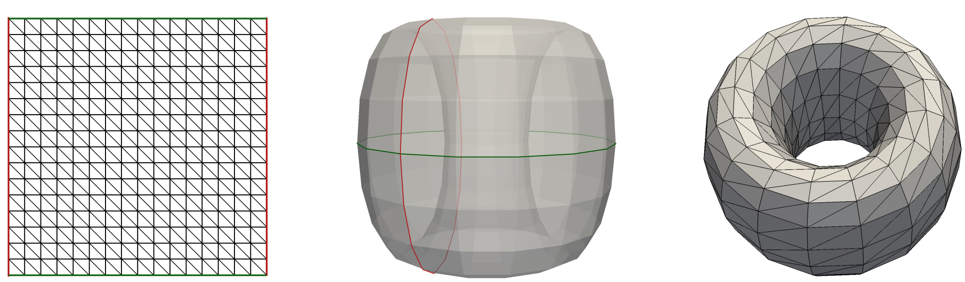

FIGURE 7. Generating the triangulation of a torus: On a uniform triangulation of $(0, 2\pi)^2$ we identify the nodes on the left with the ones on the right (red lines) and the nodes on the top with the ones on the bottom (green lines). We plot the obtained stretched torus for $\ell = 4$, $r = 1$ and $R = 2$ and the two identification lines (middle) as well as the resulting mesh (right).

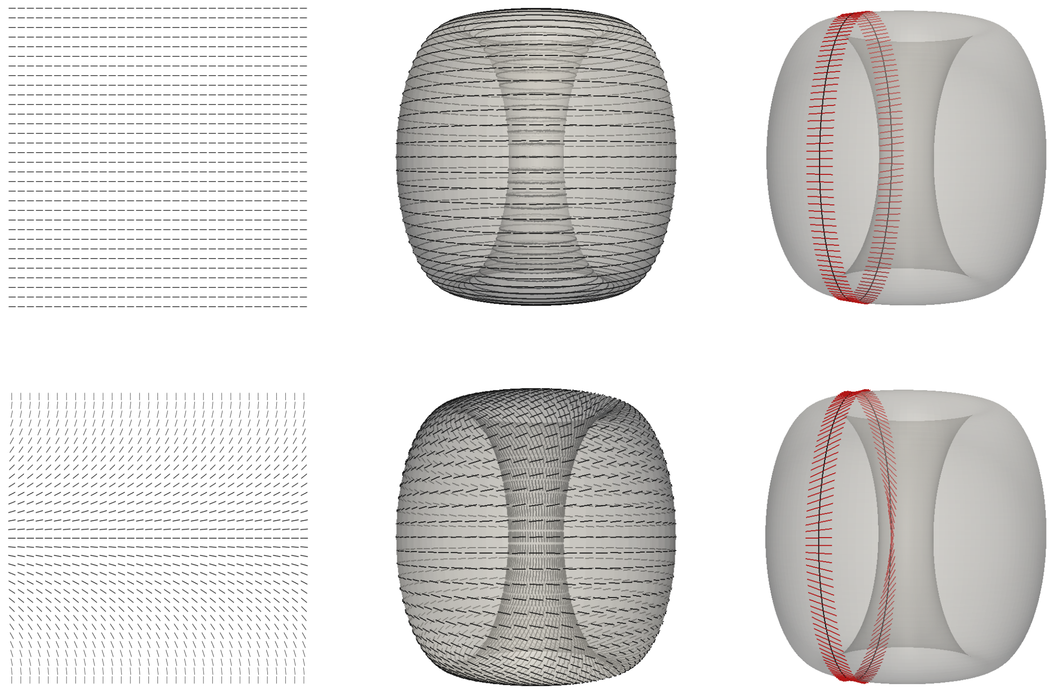

FIGURE 8. Initial data for the torus experiments: On the fundamental domain $(0, 2\pi)^2$ of $\mathbb{T}^2$ we plot the line fields $Q^0_{h,1}$ and $Q^0_{h,2}$. Since $Q^0_{h,2}$ is a Moebius strip in one direction the resulting line field on the torus is non-orientable.

where $||DX||_{L^\infty} := \max_{ij} ||\partial_i X_j||_{L^\infty} = \max\{R + r, 2.5r\}$. On $\mathbb{T}^2_h$ we define the discrete tangent vector fields

$$\begin{aligned}\tilde{n}^0_{h,1} &:= \mathcal{I}_h[\tau_2 + \text{rand}] \\ \tilde{n}^0_{h,2} &:= \mathcal{I}_h[\sin(\varphi/2)\tau_1 + \sin(\varphi/2)\tau_2 + \text{rand}],\end{aligned}$$

where rand : $\mathbb{T}^2_h \to \mathbb{R}^3$ takes random values in $(-0.1, 0.1)^3$ and φ denotes the horizontal angle in the torus coordinates defined by the parametrization X. To obtain a vector field that is tangential and has unit length at the nodes we define $\overline{n}^0_{h,i} := \mathcal{I}_h[\tilde{n}^0_{h,i} - (\tilde{n}^0_{h,i} \cdot \nu)\nu]$ for $i = 1, 2$ and then the initial data

$$n^0_{h,i} := \mathcal{I}_h \left[\frac{\overline{n}^0_{h,i}}{|\overline{n}^0_{h,i}|} \right] \quad \text{for} \quad i = 1, 2.$$

As can be seen in Figure 8 the initial line field $Q^0_{h,1} := \mathcal{I}_h[n^0_{h,1} \otimes n^0_{h,1}]$ is orientable while $Q^0_{h,2} := \mathcal{I}_h[n^0_{h,2} \otimes n^0_{h,2}]$ is a Moebius strip rotated around the x_3-axis and, therefore, non-orientable.

6.3.1. *Different ratios R/r.* Since E_{LdG} and the corresponding Euler-Lagrange equations are invariant under a rescaling $x \mapsto \lambda x$ for $\lambda > 0$ on twodimensional surfaces stationary points computed by a gradient flow algorithm only depend on the initial data Q^0 and the ratio R/r of the two radii that define the torus. We start the investigation of tangential line fields by computing final energies for the starting values $Q^0_{h,1}, Q^0_{h,2}$ and different ratios R/r. As can be seen in Figure 9 on the right for $R/r > 2$ and our choice of the initial data the energies of the final states in the class of orientable line fields is much smaller than the energies of the non-orientable configurations. We will have a closer look at the ratio $R/r = 1.5$ where the energies are of comparable size and discuss properties of the stable orientable and non-orientable line fields.

6.3.2. *Analyzing the tilt for $R/r = 1.5$.* The interest for physicists and engineers involved in the construction of bistable and multistable devices is the difference in the tilt of the liquid crystal molecules in stable configurations. The tilt of the liquid crystal molecules has an impact on polarized light crossing the device possibly leading to a new polarization. A polarizer at the end of the device measures the deviation of the

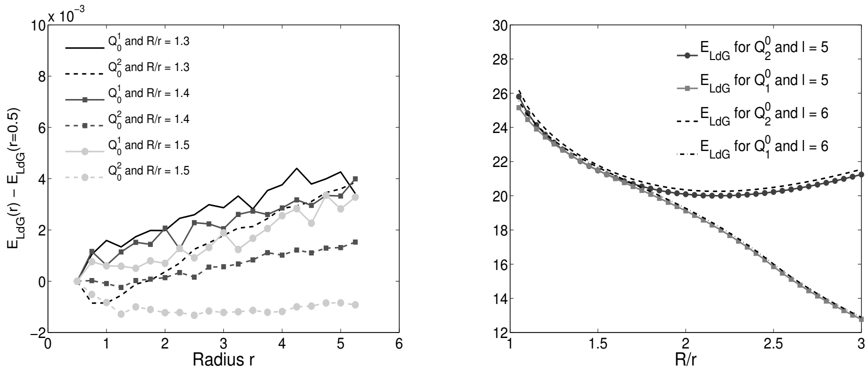

FIGURE 9. Numerically confirmed invariance of the energy E_{LdG} under a rescaling $x \mapsto \lambda x$ of the surface (left) and final energies for ratios $R/r \in (1.05, 3)$ and two meshes (right). On the left we plot $E_{LdG}(r) - E_{LdG}(r = 0.5)$ for the ratios $R/r = 1.3$,1.4 and 1.5 and initial data $Q^0_{h,1}$ and $Q^0_{h,2}$. On the right we plot the final energies for $r = 1$ and initial data $Q^0_{h,1}$ and $Q^0_{h,2}$. Note, that the energies of the final states in the class of orientable line fields is much smaller than the energies of the non-orientable final states for $R/r > 2$ and they are of comparable size for $R/r \sim 1.5$.

outgoing from the ingoing polarization. Since the polarizer passes light of a specific polarisation, say the ingoing one, regions of different polarisations due to tilted molecules appear as darker spots.

For a ratio $R/r = 1.5$ and a refinement step $\ell = 6$ we compute stationary points of E_{LdG} using orientable and non-orientable initial data $Q^0_{h,1}$ and $Q^0_{h,2}$, respectively. We measure the tilt of the molecules in terms of the x_3-component $Q_{h,33}$ of the line field. While the tilt of the crystal is almost the same on the inner part of the torus for orientable and non-orientable stable configurations we observe a difference on the outer part, see Figure 10 and Figure 11. We color all surfaces and line fields by $Q_{h,33} = |n^Q_{h,3}|^2$. In contrast to common bistable devices where different tilts of the crystal are obtained with defect and non-defect states [11, 17] we discuss, here, different stable configurations under the notion of orientability and non-orientability.

Acknowledgments. The authors acknowledge support by the DFG through the Collaborative Research Center (SFB) 611 *Singular Phenomena and Scaling in Mathematical Models.*

References

[1] Alouges, F. Liquid crystal configurations: the numerical point of view. In *Progress in partial differential equations: the Metz surveys, 3*, vol. 314 of *Pitman Res. Notes Math. Ser.* Longman Sci. Tech., Harlow, 1994, pp. 3–17.
[2] Alouges, F. A new algorithm for computing liquid crystal stable configurations: the harmonic mapping case. *SIAM J. Numer. Anal. 34*, 5 (1997), 1708–1726.
[3] Alouges, F., and Ghidaglia, J. M. Minimizing Oseen-Frank energy for nematic liquid crystals: algorithms and numerical results. *Ann. Inst. H. Poincaré Phys. Théor. 66*, 4 (1997), 411–447.
[4] Ball, J. M., and Zarnescu, A. Orientability and energy minimization for liquid crystal models. *Mol. Cryst. Liq. Cryst. 495* (2008), 573–585.
[5] Bartels, S. *Finite element approximation of harmonic maps betweeen surfaces.* Habilitation thesis, Humboldt Universität zu Berlin, Berlin, Germany, 2009.
[6] Bartels, S. Numerical analysis of a finite element scheme for the approximation of harmonic maps into surfaces. *Math. Comp. 79*, 271 (2010), 1263–1301.
[7] Bartels, S. Finite element approximation of large bending isometries. *SFB-preprint no. 501* (2011).
[8] Bartels, S., Dolzmann, G., Nochetto, R., and Raisch, A. Finite element methods for director fields on flexible surfaces. *Interfaces Free Bound. 14*, 2 (2012), 231–272.
[9] Ciarlet, P. G. *The finite element method for elliptic problems*, vol. 40 of *Classics in Applied Mathematics.* Society for Industrial and Applied Mathematics (SIAM), Philadelphia, PA, 2002. Reprint of the 1978 original [North-Holland, Amsterdam; MR0520174 (58 25001)].
[10] de Gennes, P.-G., and Prost, J. *The Physics of Liquid Crystals (International Series of Monographs on Physics)*, 2 ed. Oxford University Press, USA, 1995.

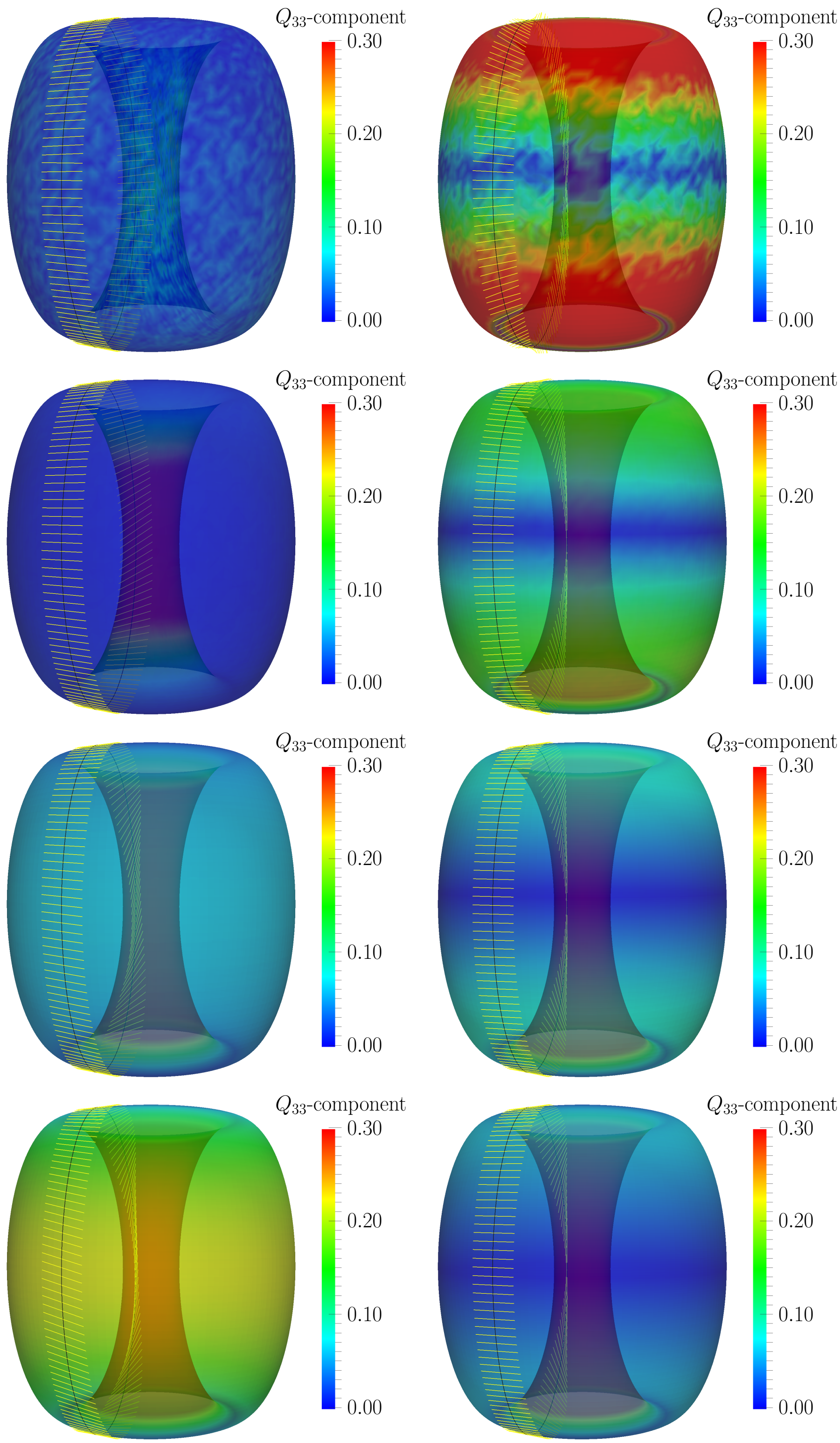

FIGURE 10. Stationary points of E_{LdG} in the class of orientable (left column) and non-orientable (right column) tangential line fields on the torus: Snapshots of the evolution under the gradient flow with initial data $Q^0_{h,1}$ (left) and $Q^0_{h,2}$ (right). On the outer part of the torus we see different tilts of the liquid crystal when the evolution becomes stationary. We color the surface by $Q_{h,33} = |n^Q_{h,3}|^2$, where the color blue corresponds to $Q_{h,33} = 0$, that is, the molecules of the liquid crystal lie in a plane orthogonal to $e_3 = [0, 0, 1]^T$.

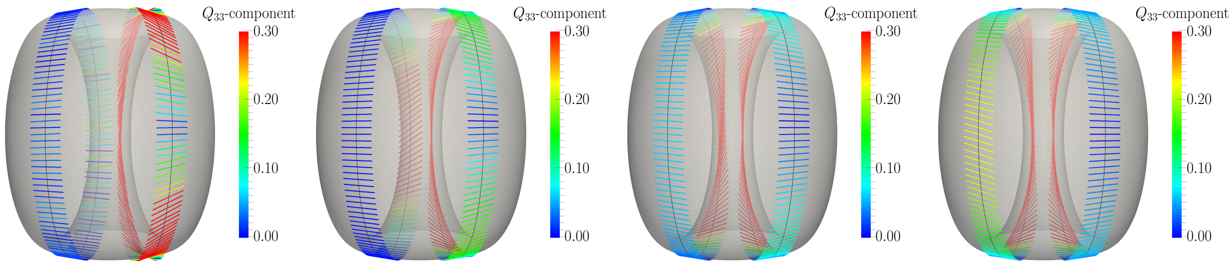

FIGURE 11. Stationary points of E_{LdG} in the class of orientable (right) and non-orientable (left) tangential line fields on the torus: We plot snapshots of a cut through the line fields and color it by $Q_{h,33}$.

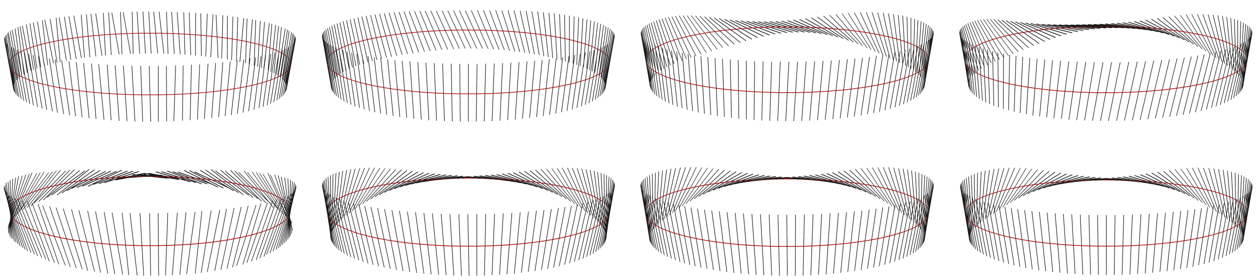

FIGURE 12. Stationary points of E_{LdG} in the class of orientable (upper row) and non-orientable (lower row) tangential line fields on the torus: Some more snapshots of a cut through the line field. All observed stationary points in the torus experiments are rotational symmetric with respect to the x_3-axis.

[11] JONES, J. C. 40.1: Invited paper: The zenithal bistable device: From concept to consumer. *SID Symposium Digest of Technical Papers 38*, 1 (2007), 1347–1350.
[12] LESLIE, F. M. Theory of flow phenomena in liquid crystals. *Advances In Liquid Crystals 4* (1979), 1–81.
[13] LIN, F., AND LIU, C. Static and dynamic theories of liquid crystals. *J. Partial Differential Equations 14*, 4 (2001), 289–330.
[14] MAJUMDAR, A., AND ZARNESCU, A. Landau-De Gennes theory of nematic liquid crystals: the Oseen-Frank limit and beyond. *Arch. Ration. Mech. Anal. 196*, 1 (2010), 227–280.
[15] PERSSON, P.-O., AND STRANG, G. A simple mesh generator in Matlab. *SIAM Rev. 46*, 2 (2004), 329–345 (electronic).
[16] RAISCH, A. *Finite Element Methods for Geometric Problems.* Phd thesis, Rheinische Friedrich-Wilhelms Universität Bonn, Bonn, Germany, 2012.
[17] UCHE, C., ELSTON, S. J., AND PARRY-JONES, L. A. Microscopic observation of zenithal bistable switching in nematic devices with different surface relief structures. *Journal of Physics D: Applied Physics 38*, 13 (2005), 2283.
[18] VIRGA, E. G. *Variational theories for liquid crystals*, vol. 8 of *Applied Mathematics and Mathematical Computation.* Chapman & Hall, London, 1994.

UNIVERSITÄT FREIBURG, ABTEILUNG FÜR ANGEWANDTE MATHEMATIK, HERMANN-HERDER-STR. 10, D-79104 FREIBURG, GERMANY

UNIVERSITÄT BONN, INSTITUT FÜR NUMERISCHE SIMULATION, WEGELERSTR. 6, D-53115 BONN, GERMANY